Layer-by-Layer Assembled Electrochromic Films for All-Solid-State Electrochromic Devices

Eunkyoung Kim* and Soonkyo Jung

Department of Chemical Engineering, Yonsei University, 134 Sinchon-dong, Seodaemun-gu, 120-749, Seoul, Korea

Received July 11, 2005. Revised Manuscript Received October 6, 2005

A layer-by-layer (LBL) assembled electrochromic (EC) film was investigated by using poly(aniline-*N*-butylsulfonate)s (PANBS) as an electrochromic anionic polymer, and acid-doped polyaniline (PAN) and vinylbenzyldimethyl-*n*-octadecylammonium salts (VBOD) as a polycation. The layer sequence of the EC films was varied to optimize EC properties by changing the order of layer deposition. Electrochemical and electrochromic properties of EC films were highly dependent on the layer sequence. In the EC film composed alternatively of the PANBS/PAN and PANBS/VBOD bilayers (L1), higher redox current density was observed than that of the EC film composed conductive PANBS/ PAN layers. Furthermore, optical change (ΔOD) between the colored and the bleached state was largest in L1 among the EC films assembled in this study. This indicates that charge transport in L1 is more facile, reducing interlayer barrier (ILB) energy for charge transfer, possibly due to the flexible long alkyl chains of VBOD that may facilitate ion transport. An all-solid-state EC device based on an optimized LBL composition showed an EC response at 3 V within 1 s, with a stable memory effect.

Introduction

Electrochromic (EC) devices have attracted much interest due to their low power consumption as well as their memory effect.[1] Much progress has been made in developing new materials that exhibit long-term stability and various colors at different potentials, and in fabricating through nanotechnology.[2] Within nanofabrication, the electrostatic layer-by-layer (LBL) assembly technique[3] has been introduced to fabricate EC electrodes to allow precise control of polymer assembly and to create an ideal tool for tailoring the properties of electroactive polymer films on the nanometer scale by electrostatic deposition of polycation and polyanion. Thus, LBL assembly based on complementary coloring electrodes have been reported, using poly(3,4-ethylene dioxythiophene) (PEDOT) and polyaniline,[2b] or a sulfonated PEDOT,[2c] an alkylsufonated polyaniline,[4] and inorganic electrochromic systems such as transition metal complexes and poly(oxometalates).[5] In these examples, an inert polymer such as poly(diallyl dimethylammonium chloride) (PDAC), poly(allylamine hydrochloride) (PAH), poly(acrylic acid) (PAA), poly(styrene sulfonate) (SPS), or an inert alkyl ion such as vinylbenzyldimethylalkylammonium chloride (VBDAC)[4] is used as the counterpolyion for the electroactive species.

From a practical point of view, all-solid-state EC devices would be desirable.[1c] Reports on an all-solid-state EC device fabricated with an EC layer in contact with a solid-state electrolyte layer such as polymer electrolyte membrane, however, are rare.[4,6] Furthermore, charge and ion transport in a multilayered film assembled by nanoengineering is not well-understood. Uncertainty remains regarding the building model in a multilayered electrochromic device and a more generally nanoassembled electrochemical device.

It is generally known that charge transport in amorphous organic materials occurs via thermally activated hops, with a mobility that typically increases with both electric field and temperature.[7] Thus, the electron transfer rate is highly dependent on the distance between the donor and the acceptor. A multilayered system that has an electrically resistive counterionic layer between the EC layers can increase the distance between the electroactive layers and decelerate the electrochromic response. In this context, it is important to reduce the gap generated by the electrically resistive counterionic layer so electron tunneling can be made possible through the gap. On the other hand, building with electroactive layers that have conductive counterions within the LBL film is also an interesting and ideal system to use to study electron transport between the layers. Conductive countercations, however, often yield poor layering due to

* To whom correspondence should be addressed. Tel: 82-2-2123-5752. Fax: 82-2-312-6401. E-mail: eunkim@yonsei.ac.kr.

(1) (a) Platt, J. R. J. *J. Chem. Phys.* **1961**, *34*, 862. (b) Mortimer, R. J. *Chem. Soc. Rev.* **1997**, *26*, 47. (c) Grätzel, M. *Nature* **2001**, *409*, 575. (d) Ahn, K.-S.; Nah, Y.-C.; Park, J.-Y.; Sung, Y.-E.; Cho, K.-Y.; Shin, S.-S.; Park, J.-K. *Appl. Phys. Lett.* **2003**, *82*, 3379. (e) Cho, S. I.; Kwon, W. J.; Choi, S.-J.; Kim, P.; Park, S.-A.; Kim, J.; Son, S. J.; Xiao, R.; Kim, S.-H.; Lee, S. B. *Adv. Mater.* **2005**, *17*, 171.

(2) (a) Peters, A.; Branda, N. R. *J. Am. Chem. Soc.* **2003**, *125*, 3404. (b) DeLongchamp, D.; Hammond, P. T. *Adv. Mater.* **2001**, *13*, 1455. (c) Cutler, C. A.; Bouguettaya, M.; Reynolds, J. R. *Adv. Mater.* **2002**, *14*, 684. (d) Argun, A. A.; Aubert, P.-H.; Thompson, B. C.; Schwendeman, I.; Gaupp, C. L.; Hwang, J.; Pinto, N. J.; Tanner, D. B.; MacDiarmid, A. G.; Reynolds, J. R. *Chem. Mater.* **2004**, *16*, 4401.

(3) Decher, G. *Science* **1997**, *277*, 1232.

(4) Jung, S.; Kim, H.; Han, M.; Kang, Y.; Kim, E. *Mater. Sci., Eng. C* **2004**, *24*, 57.

(5) (a) Millward, R. C.; Madden, C. E.; Sutherland, I.; Mortimer, R. J.; Fletcher, S.; Marken, F. *Chem. Commun.* **2001**, 1994. (b) Liu, S. Q.; Kurth, D. G.; Mohwald, H.; Volkmer, D. *Adv. Mater.* **2002**, *14*, 225.

(6) Kim, E.; Lee K.; Rhee, S. B. *J. Electrohem. Soc.* **1997**, *144*, 227.

(7) Baldo M. A.; Forrest, S. R. *Phys. Rev. B* **2001**, *64*, 085201.

10.1021/cm051492n CCC: $30.25
Published on Web 11/15/2005

Chart 1. Chemical Structure of Layer Composition

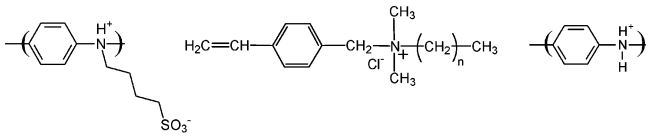

PANBS **VBOD (n=17)** **PAN**

their irregular and granular structures. Furthermore, the color contrast of EC films with conductive cation layers could be small due to the color development of the cation itself upon oxidation or doping, as observed often in polyaniline. In addition, ion transport in an EC layer could be an important issue for EC reaction that requires counterion balancing accompanied by the redox reaction. Thus, it is necessary to build an EC layer with a mixed ionic (e-conductive and ion conductive, but transparent) composition to obtain an all-solid-state EC device with high color contrast and faster response.

Herein, we report the combination of layering materials in assembling EC films and the effect of layer sequence in layer-by-layer assembled conducting polymer films on the EC properties of an all-solid-state EC device. As an alkylsulfonated polyaniline offers high redox stability as well as electrochromic and self-assembling properties,[8−10] poly(aniline-*N*-butylsulfonate)s (PANBSs) were adopted as the electroactive anionic polymers for the layering. The counterions for the PANBS layers were polyaniline (H^+-doped) and vinylbenzyldimethyl-*n*-octadecylammonium salts (VBOD) as the polycation. The structures are given in Chart 1.

Experimental Section

Materials. Methoxy poly(ethylene glycol) 1000 monomethacrylate (MPEGM) was purchased from Polyscience Inc. Triallyl-1,3,5-triazine-2,4,6-(1*H*,3*H*,5*H*)-trione (TATT, Aldrich) was used as a cross-linker. Poly(ethylene glycol) dimethyl ether (PEGDMe, M_w = 330) was purchased from Aldrich and was purified by distillation before use. Lithium trifluoromethanesulfonate ($LiCF_3SO_3$) was purchased from Merck. Darocure 1173 (Ciba Specialty Chemicals) was used as a photocuring agent. TiO_2 (Degussa P25, diameter = 21 nm) was dried in a vacuum oven at 150 °C for 15 h before it was used. Sodium persulfate was obtained from Aldrich. VBOD was synthesized according to ref 11. Aniline *N*-butanesulfonic acid was prepared as previously reported.[6,8−10] Chemical polymerization was carried out in a reaction vessel at 0 °C using sodium persulfate as an oxidant.[12,13] Electrochemical deposition of PANBS was performed on an ITO glass using a solution of aniline-*N*-butane sulfonate in acetonitrile containing 5% (wt) $HClO_4$.[6] The thickness of the electrochemically synthesized PANBS film was 300 nm as determined by an alpha step.

Chart 2. Layer Sequence of LBL Assembled Electrochromic Films

L1 = |○|X|○|X|○|X|○| L2 = |○|○|X|○|○|X|○|

L3 = |○|○|○|X|○|○|○| L4 = |○|X|X|○|X|X|○|

L5 = |○|○|○|○|○|○|○| L6 = |X|X|X|X|X|X|X|

| = PANBS; ○ = PAN; X = VBDO

Preparation of Polymer−Salt Membrane. MPEGM (2.5 g), TATT (0.3 g), PEGDMe (2.5 g), and Darocure 1173 (0.25 g) were mixed in a dark glovebox using a magnetic stirrer. $LiCF_3SO_3$ (0.25 g) was dissolved in the aforementioned mixture ([EO]/[Li] = 12.5), and the resulting mixture was mixed with TiO_2 (10 wt % of the aforementioned mixture). The mixture was stirred vigorously for 1 day to yield a radical, curable electrolyte solution.

LBL Self-assembly of PANBS. PANBS was dissolved in water at a concentration of 2 mg/mL. An aqueous solution of VBOD was prepared at the same concentration. Undissolved particles were filtered using a filter paper. ITO glass (SHOTT Korea, ~10 Ω) was treated with *N*-(2-aminoethyl)-3-aminopropyl-trimethoxysilane to make the substrate surface hydrophilic. A multilayered film was obtained by alternatively dipping the ITO glass into a 0.2 wt % PANBS aqueous solution and a polycation solution (PAN or VBOD, 2 mg/mL) for 10 min using a homemade dipper that controls the dipping speed. The electrochromic PANBS layer (I) was deposited first as an anionic layer and then PAN (○) or VBOD (×) as a countercation layer to produce a bilayer, which was built in sequence. The order, however, was modified as shown in Chart 2.

Every odd-numbered layer corresponds to PANBS and every even-numbered layer to the countercation (either PAN or VBOD). The total number of layers in each film was the same (15 layers) and the first layer of each film was PANBS, so the interfacial barrier ITO/PANBS for the electron transfer would be the same for all the films. The LBL film was dried with nitrogen gas after washing with distilled water. The drying procedure between the adsorption of either cationic or anionic layers was necessary for building uniform, self-assembled layers.

All-Solid-State Electrochromic Device (ECD). All-solid-state ECDs were assembled by placing the photopolymerizable electrolyte mixture, described above, between the PANBS-coated ITO glass and the bare ITO glass (counter electrode). The spacing between those two faces was controlled by placing an insulating polyimide tape (50 μm) on the ITO glass. The above photopolymerizable electrolyte mixture was injected between the PANBS/VBOD-LBL-film-coated ITO glass and the bare ITO glass. The EC device was irradiated for 1 h at 365 nm using a UV lamp (Spectronics Company Model ENF-280C) to prepare solid polymer electrolyte through radiation curing of the photopolymerizable electrolyte. All the samples were handled in a glovebox. The area of the devices was 1 × 1 cm^2 for EC property characterizations but 5 × 10 cm^2 for a patterned device (Figure 8).

Instrumentation. The in situ spectroelectrochemical system consisted of a computer-controlled reflectance spectrophotometer using an Ocean Optics S-2000 fiber optic spectrometer and an electrochemical subsystem (BAS 100B). CV was obtained by BAS 100B. The $E_{1/2}$ of the redox peaks were determined by deconvolution of the peaks assuming Gaussian mode using Orgin 6.1. Layer thickness was determined by an alpha step (TENCOR INSTRUMENTS, Alpha-step 200). Digital Instruments Nanoscope IIIa was used to obtain atomic force microscopy (AFM) images.

Results and Discussion

Film Growth by LBL Assembly. Electrochromic films were fabricated using the LBL approach, which involves the

(8) (a) Kim, E.; Lee, M.-H.; Moon, B. S.; Lee, C.; Rhee, S. B. *J. Electrochem. Soc.* **1994**, *141*, L26. (b) Kim, E.; Lee, K.-Y.; Lee, M.-H.; Shin, J.-S.; Rhee, S. B. *Synth. Met.* **1997**, *85*, 1367.
(9) Kim, E.; Lee, M.-H.; Rhee, S. B. *Synth. Met.* **1995**, *69*, 101. (b) Jang, J. H.; Kim, J.; Lee, K.; Lee, H.; Kim, E.; Rhee, S. B. *Synth. Met.* **1995**, *69*, 173. (c) Kim, E.; Lee, M.-H.; Rhee, S. B. *Mol. Cryst., Liq. Cryst.* **1997**, *295*, 77.
(10) Kang, Y.; Kim, E.; Lee, C. *Mol. Cryst. Liq. Cryst.* **2001**, *371*, 87.
(11) Fu, X.; Qutubuddin, S. *Polymer* **2001**, *42*, 807.
(12) MacDiarmid, A.; Chiang, J.; Halpern, M.; Huang, W.; Mu, S.; Somasiri, N.; Wu, W.; Yaniger, S. *Mol. Cryst. Liq. Cryst.* **1985**, *121*, 173.
(13) Krause, S.; Bohon, K. *Macromolecules* **2001**, *34*, 7179.

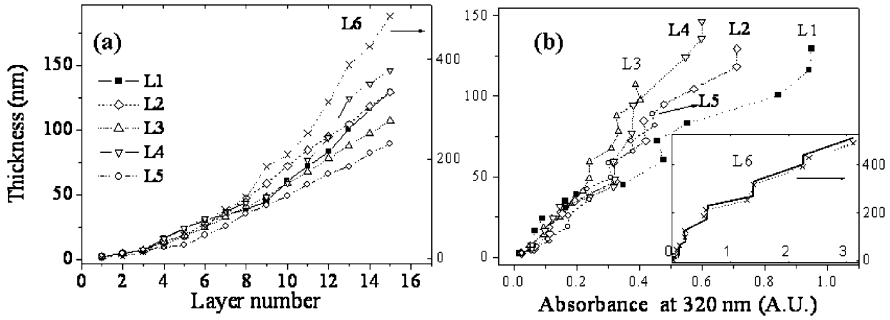

Figure 1. (a) Growth of the layer thickness as a function of the number of layers in the EC films. (b) Plot of the layer thickness growth against absorbance increase at 320 nm.

dipping of a clean ITO glass substrate in dilute aqueous solutions of polycation and polyanion in an alternating manner, followed by rinsing between each deposition step.[14] The layer thickness of the film increased as the layer number was increased, as shown in Figure 1. The growth was almost a linear profile for L1−L3, and for L5 to the 15th layer, with the growth of 2−7 nm per layer. L4 showed a deviation from linearity, and L6 could be fitted into an exponential growth profile with a relation of d (nm) = 25 exp(n/4.9), where d is the thickness of the film and n the layer number. Such nonlinear growth profiles in polyelectrolyte LBL films are a well-established phenomenon, and explanations of the exact exponential assembly mechanism vary. One explanation, offered for high-ionic-strength deposition, suggests that the superlinear growth is due to the increased surface roughness, which in turn presents an increasing surface area that permits the deposition of increasing amounts of material.[15]

UV−vis spectroscopy was used to monitor the growth of the LBL films on ITO glasses. In our previous study, the spectral growth by UV spectroscopy for the PANBS assembly was correlated to the mass increase on the electrode, as determined by EQCM.[10] Taking L6 film as an example, the UV−vis spectra at consecutive cycles showed that the absorption band increased with the number of layers. Figure 1b shows a correlation between the thickness growth and the absorbance increase at 320 nm for L1−L6 at different layer numbers. The absorbance at selected wavelength increased as the number of PANBS layers (odd-numbered layers) were increased, indicating homogeneous growth of the layers without detachment nor phase separation between the dipping process. The accumulation of VBOD layer did not significantly affect the spectral change, as shown in Figure 1b (inset), for L6, since VBOD does not absorb in this spectral region. On the other hand, visible spectral change for L1−L5 upon layer growth reflected the absorbance increase arising from both PANBS and PAN. This confirms that the multi-bilayer films are built up by the electrostatic interaction. Importantly, the absorbance increase (and thickness growth) of PANBS was highly dependent on the layer composition, indicating different affinities of PANBS for different cations. As the absorbance increase of L6 was much larger than that of L5, it can be concluded that the affinity of PANBS with VBOD is stronger than that with PAN.

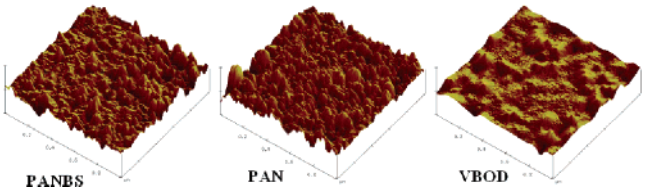

Figure 2. Surface morphology for PANBS, PAN, and VBOD surface by AFM: (a) ITO (bottom)/(PANBS/PAN)2/PANBS (top), (b) ITO/(PANBS/PAN)2/PANBS/PAN (top), and (c) ITO/(PANBS/VBOD)2/PANBS/VBOD (top).

Figure 2 represents the film morphology for three different films assembled with the following order: (a) ITO (bottom)/$(PANBS/PAN)_2$/PANBS (top), (b) ITO/$(PANBS/PAN)_2$/PANBS/PAN (top), and (c) ITO/$(PANBS/VBOD)_2$/PANBS/VBOD (top). The scale is 1 μm. The roughness and thickness can depend on the drying procedure, but the granular morphology is maintained, as reported for polyaniline films obtained with other techniques.[16] Globular morphology was observed from the PAN surface (Figure 2b) with surface roughness (root-mean-square) of 1.30 nm, and the distribution of the grain was more uniform compared to that of PANBS (Figure 2a). On the other hand, VBOD morphology was structureless (Figure 2c), and the AFM image of the VBOD surface reflected the image of the PANBS surface coated underneath it. The surface roughness was decreased from 1.65 to 0.94 nm as a result of the VBOD coating on PANBS. This result indicates that the exponential growth in L6 could be attributed to the roughness increase in PANBS, which forms a large globular morphology. Regardless of the assembly mechanism, films with this architecture device have unique electrochromic properties, as described below.

Cyclic Voltammetry (CV). CV was used to identify the redox potential ranges and to elucidate the general electrochemical behavior of the electrochromic layer. PAN and PANBS have different redox potentials, and VBOD does not have a redox property in the scanning range between −0.5 and 2.0 V vs Ag/AgCl, in a supporting electrolyte containing 0.1 M of $LiClO_4$ and 5% of $HClO_4$ in CH_3CN (scan rate of 50 mV/s). The color of the EC films was changed from transparent yellow to deep green as the potential was raised to 0.5 V and intensified above 0.7 V and then bleached under the potential below 0.1 V. Figure 3 shows CV applied to

(14) (a) Decher, G.; Hong, J. D. *Makromol. Chem., Macromol. Symp.* **1991**, *46*, 321. (b) Lvov, Y.; Haas, H.; Decher, G.; Möhwald, H.; Mikhailov, A.; Utchedlishvily, B.; Morgunova, E.; Vainshtein, B. *Langmuir* **1994**, *10*, 4232.

(15) Ruths, J.; Essler, F.; Decher, G.; Riegler, H. *Langmuir* **2000**, *16*, 8871.

(16) Porter, T. L. *Surf. Sci.* **1993**, *293*, 81.

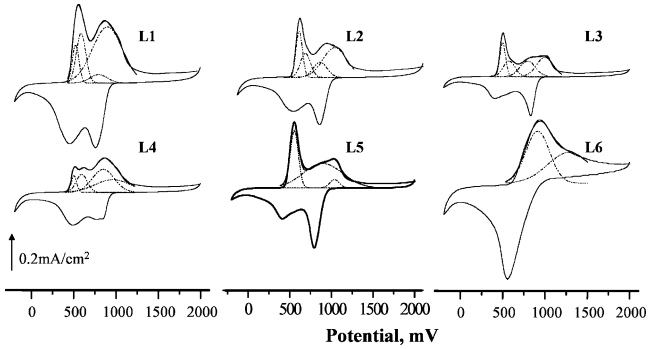

Figure 3. Cyclic voltammogram of EC films in a supporting electrolyte containing 0.1 M of $LiClO_4$ and $HClO_4$ in CH_3CN, with a scan rate of 50 mV/s. Dotted lines are the peaks obtained from the deconvolution of the oxidation curve assuming Gaussian modes.

the multilayer-coated ITO glass surface. Two sets of redox peaks are observed with the $E_{1/2}$ at 0.74 and ~0.9 V for L6, where the film consisted of PANBS/VBOD. The peaks could be ascribed to the one-electron (1-e) and two electron (2-e) redox process of PANBS, respectively, albeit those are slightly shifted to higher potentials compared to those in different electrolyte systems.[6,8−10] The full-width at half-maximum (fwhm) and the peak separation between the oxidation and reduction (370 mV) are much larger than the value expected for an ideal 1-e Nernstian redox system, indicative of the repulsive interactions of the redox sites.[17] This is mainly due to the presence of the electrically resistive VBOD layers between the PANBS layers. Although VBOD is resistive toward electron transfer, it seems to be ion conductive to transfer counterions, to result in reversible CVs over several repetitive cycles.

The CV for L5 showed more than two sets of redox peaks with the $E_{1/2}$ at 0.48, 0.70, and 0.93 V (Figure 3, L5). The first two peaks at 0.48 and 0.69 V could be assigned as the 1-e redox process of PAN (emeraldine/leucoemeraldine) and PANBS, respectively, based on the above result for L6 and previous report.[18] The peak separation and fwhm of the 1-e process for PAN were much smaller than those of PANBS, indicating that the electron conductivity of PAN is larger than that of PANBUS. Furthermore, 1-e redox potential for PANBS was shifted to a lower value with decreased peak separation. This result indicates that the charge propagation through the consecutive PANBS layers takes place more easily between the adjacent PAN layers than in the VBOD layer, which is electrically resistive. The third peak at 0.93 V may be assigned as the overlap of the 2-e redox process of PAN (emeraldine/pernigraline) and that of PANBS.

In the EC films containing both PAN and VBOD layers as the countercationic layer (Figure 3, L1−L4), more complicated redox peaks were observed with different $E_{1/2}$ values and current density depending on the layer sequence. This result strongly indicates that the layer sequence affects the redox process in the EC films. The 1-e redox peak of PAN at ~0.45 V was observed at a similar potential as those observed for the PANBS/PAN film (L5). The 1-e redox peaks of PANBS for different films could not be clearly resolved due to the peak complexity and heavy overlapping of the peaks. However, a broad peak at ~0.7 V could be assigned as the 1-e redox peak of PANBS based on the CV of L5 and L6. The redox peak at ~0.7 V might be the overlapped one with the 2-e process of PAN and of PANBS but separated partly in L2 and L3 from the peaks of the 2-e process.

Interlayer Barrier (ILB) Energy for Charge Transfer in LBL Films. Interestingly, L4 showed a new resolved peak at ~0.6 V, which could be originated from a new energy barrier relating to interfacial charge/ion transport. Since acidity is generally very weak and almost constant in organic solvents such as CH_3CN, the new peak is unlikely ascribed to the peak separation of PAN reported in an acidic condition.[19] Furthermore, it would not be ascribable to the 1-e redox peak of PANBS because the peak is much sharper than the redox peak of PANBS. Therefore, we may assign the new peak at ~0.6 V as the potential generated by the two adjacent bilayers of the PANBS/VBOD of L4.

As the VBOD layer is more electrically resistive but ion conductive than the conducting polymers (PAN and PANBS), it can generate junction potential differences at the interface between the double PANBS/VBOD layers that are in contact with the PANBS/PAN layers, similar to the Donnan potential differences present at the interface between the polyelectrolyte coatings on the electrodes and electrolyte solutions.[20] Generally, in a double-junction structure, if each junction resistance is much higher than the quantum unit of resistance ($R_Q \sim 26$ kΩ) due to a long electron-tunneling distance or a high tunneling barrier, the electron transport occurs in two independent sequential steps, with possible occupation of the molecular tunneling bridge.[21] It is rather a complex problem to distinguish such a junction resistance (or interlayer barrier) through the multilayers for each EC film with our limited data. However, the appearance of a new peak in L4 and peak broadening in the CV of L1−L3 indicates a new energy state with apparent formal potential, which would be qualitatively related to the separation of the conducting layers, as described below.

Since the first peak belongs to PAN, it can be assumed that the electron transfer from the PAN layer of PANBS/PAN to the next level (PANBS/PAN) would be more favorable when the film does not contain a VBOD layer. In L1−L3, only one VBOD layer is intercalated between the two PAN layers, while in L4, two VBOD layers are intercalated. Therefore, the potential shift toward a high potential in L4 would be larger than that in the other mixed cationic films (L1−L3) because the two adjacent VBOD

(17) Bard, A. J.; Faulkner, L. R. *Electrochemical Methods. Fundamentals and Applications*, 2nd ed.; Wiley: New York, 2001.
(18) Huang, W.-S.; Humphrey, B. D.; MacDiarmid, A. G. *J. Chem. Soc., Faraday Trans. 1* **1986**, *82*, 2385. (b) Baba, A.; Tian, S. J.; Stefani, F.; Xia, C. J.; Wang, Z. H.; Advincula, R. C.; Johannsmann, D.; Knoll, W. *J. Electroanal. Chem.* **2004**, *562*, 95. (c) Tian, S.; Liu, J.; Zhu, T.; Knoll, W. *Chem. Mater.* **2004**, *16*, 4103.
(19) Qi, B.; Lu, W.; Mattes, B. R. *J. Phys. Chem. B* **2004**, *108*, 6222.
(20) (a) Likharev, K. K. *Proc. IEEE* **1999**, *87*, 606. (b) Zhao, J.; Uosaki, K. *J. Phys. Chem. B* **2004**, *108*, 17129.
(21) (a) Naegeli, R.; Redepening, J.; Anson, F. C. *J. Phys. Chem.* **1986**, *20*, 6227. (b) Ugo, P.; Anson, F. C. *Anal. Chem.* **1989**, *61*, 1802. (c) Doblhofer, K.; Armstrong, R. D.; Asturias, G. E.; Jang, G.; MacDiarmid, A. G.; Zhong, C. *Ber. Bunsen-Ges. Phys. Chem.* **1991**, *11*, 1381. (d) Doblhofer, K.; Vorotyntsev, M. *Electroactive Polymer Electrochemistry. Part 1. Fundamentals*; Lyons, M. E. G., Ed.; Plenum: New York, 1994; Chapter 3, p 375.

Table 1. CV Peak Potentials (E_{ox}) and Current for Oxidation Process of LBL EC films determined by deconvolution of the corresponding CV

film	PAN[a]	VBOD[a]	E_{ox1} (V)	i_{ox1} (mA)	fwhm$_1$ (V)	E_{ox2} (V)	i_{ox2} (mA)	fwhm$_2$ (V)	E_{ox3} (V)	i_{ox3} (mA)	fwhm$_3$ (V)	E_{ox4} (V)	i_{ox4} (mA)	fwhm$_4$ (V)
L1	4	3	522	18.9	77	589	24.4	110	798	0.41	203	906	27.8	354
L2	5	2	534	22.8	76	606	11.9	118	778	0.81	149	976	15.3	317
L3	6	1	500	16.9	67	595	0.79	139	795	0.79	185	1005	0.97	198
L4	3	4	501	0.82	61	624	0.93	130	847	11.5	259	972	0.64	410
L5	7	0	544	33.7	91	649	0.95		809	0.26	94	978	16.8	326
L6	0	7							899	0.25	381	1305	15.4	505

[a] Layer number.

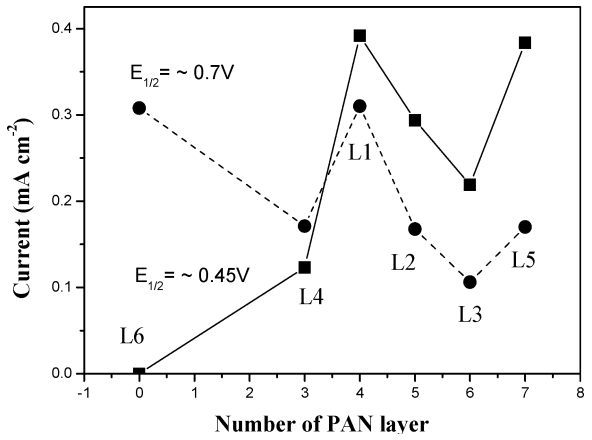

Figure 4. Oxidative current intensity after the deconvolution of the peaks in Figure 3.

layers in L4 increase the distance between the electron donor and the acceptor. Therefore, the new peak at ~0.6 V in the CV of L4 may be assigned as an interlayer barrier (ILB) arising from the two adjacent PANBS/VBOD bilayers. As the CV of L1−L3 is scrutinized, it would be observed that the first peak at ~0.5 V is much broader, possibly due to the overlapping of the two peaks: the oxidation of PAN and ILB. Two peaks can be obtained through the deconvolution of the CV peaks for oxidation (Figure 3, dotted curves, and Table 1) peak of L1−L4 in the ~0.5 V region.

Figure 4 shows oxidative current intensity after the deconvolution of the peaks in CV. The current intensities of the first two peaks decreased as the number of PAN layers decreased. In L1, however, where there were four PAN layers, the current intensities of the first peak at 0.45 V were much higher as compared to those of L2 and L3, although the total number of PAN layers in L1 was smaller than those of the latter. Such an unusual current increase in L1 may relate to the layer sequence, where the PAN and VBOD layers are alternatively assembled. According to the electron transfer theory,[22] the electron-tunneling rate constant (k') is highly dependent on the distance[23] between the donor and the acceptor (d, in this case, is the separation between the PAN layers),

$$k' = k_o \exp[-\beta(d - d_o)] \quad (1)$$

where k_o is the rate constant at contact distance d_o and β is the decay constant. The presence of one VBOD layer

Chart 3. Redox Reaction of PANBS in LBL Assembled Electrochromic Films

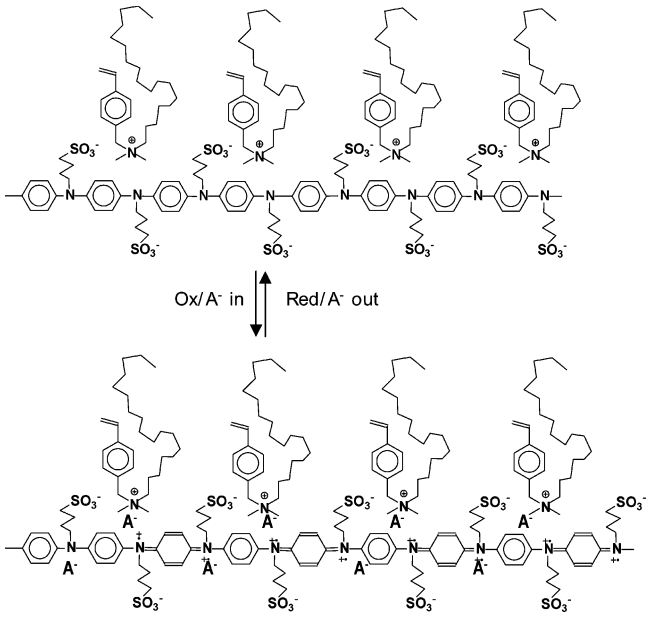

between the PAN layers could increase the distance between the PAN layers and thus deter the electron transport. Surprisingly, the current density of L1 in Figure 3 was much higher than that of L5. This indicates that charge transfer through the VBOD monolayer is effective, and that the transfer in L1 is more facile than that in L5. Such a facile electron transfer could be attributed to the presence of a long alkyl chain in VBOD, which can provide free volume around the layer, possibly facilitating ion transport, accompanied by the redox reaction, to balance the charge. In particular, the redox reaction of PANBS requires anion (A^-) transport to compensate for the positive PANBS, as described in Chart 3. Thus, facile electron transfer by PAN followed by effective ion transport through the VBOD layer seemed to be the major contribution to the high current density in L1.

As summarized in Table 1, the interlayer barrier energy (E_{ox2}) for oxidation in L1 is small, and the peak seems overlapped with E_{ox1}. Since the current intensities of the rest of the peaks (third and fourth peaks) in L1 are also high compared to those of the other mixed cationic films (L2−L4), and are even higher than those of L5 and L6, it can be assumed that electron/ion transfer for the redox reaction of the PANBS layers can also be assisted by the VBOD layer. As the intensity of E_{ox4} is larger than that of E_{ox3} in L6, E_{ox4} may be assigned for the oxidation of PANBS, and E_{ox3} for that of PAN (2e-).

Although the VBOD layer could be effective as an ion-transporting layer, the presence of two PANBS/VBOD

(22) Marcus, R. A.; Sutin, N. *Biochim. Biophys. Acta* **1985**, *811*, 265. (b) Closs, G.; Miller, J. *Science* **1988**, *240*, 440. (c) Wuttke, D.; Bjeerrum, M.; Winkler, J.; Gray, H. *Science* **1992**, *256*, 1007.

(23) (a) Moser, C. C.; Keske, J. M.; Warncke, K.; Farid, R. S.; Dutton, P. L. *Nature* **1992**, *355*, 796. (b) Laurent, D.; Schlenoff, J. B. *Langmuir* **1997**, *13*, 1552.

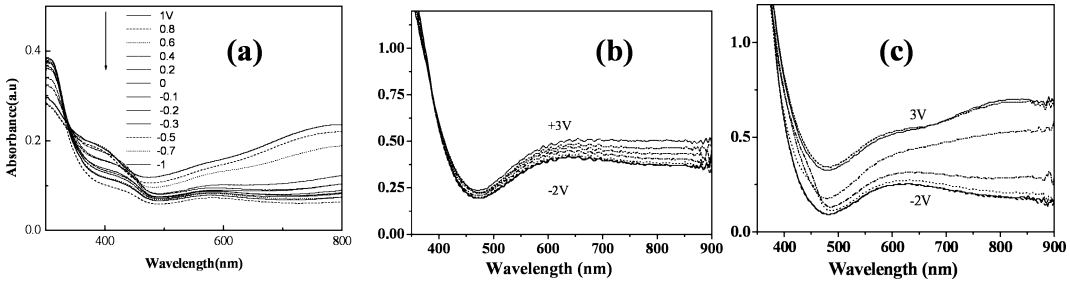

Figure 5. UV−Visible spectra of the EC films: (a) L1 in CH_3CN solution containing $LiClO_4$ and $HClO_4$. (b) L5 and (c) L1 in an all-solid-state EC devices at different applied potentials (from top to bottom: 3 V, −2 V).

Chart 4. Schematic Comparison of the Electron and Anion Transfer in (a) PANBS/PAN, Where Electrons Are Trapped through the Conductive PAN Layer; (b) L1, Where Electron Tunneling Is Possible through the VBOD Layer, and Where Anions Transport Is Facilitated by the Alkyl Chain of VBDO, Resulting in a Low Interlayer Barrier; and (c) L4, Where Electron Tunneling Is Difficult Due to the Presence of Two Resistive VBOD Layers between the PAN Layers, Resulting in a High Interlayer Barrier

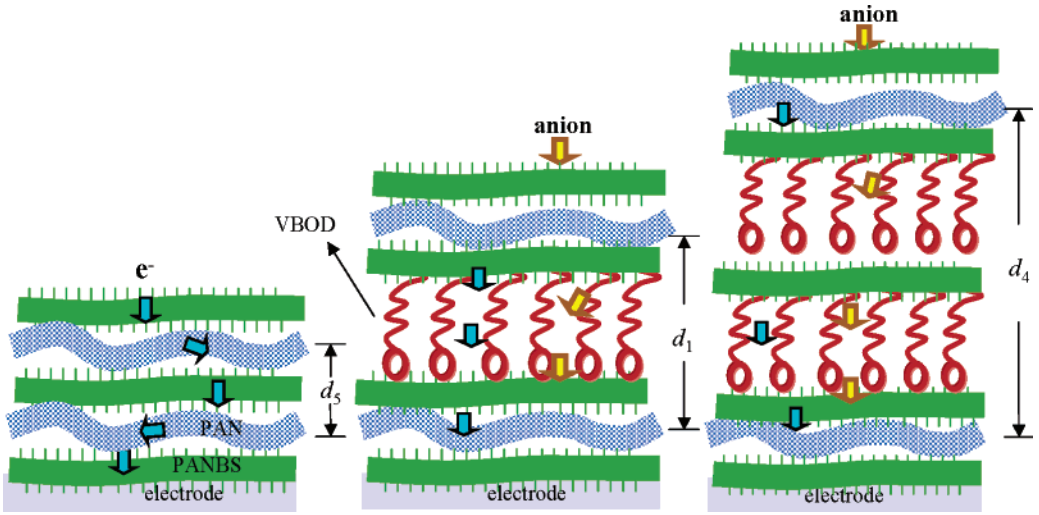

bilayers between the PANBUS/PAN bilayer in L4 increases the distance (d_4 in Chart 4) between the PAN layers, which decreases the electrochemical activity of the whole electrode. This result points out the importance of electron transport in these EC films. Unexpectedly, the current density in L5 was much smaller than that of the mixed ionic films (L1−L4). This result indicates that charge/ion may be trapped in the conductive PAN layers and that the transport becomes less efficient when the PANBS/PAN bilayers are built in sequence without ion-transporting VBOD interface. As can be seen in Figure 1a, the layer thickness of L5 is much thinner than others, indicating that the film is much more compact and there is not much room for ion transfer in L5. The charge transport process in L1, L4, and L5 are depicted in Chart 4, showing electron hopping between the PAN layers, a VBOD channel for the counterions, and electron trapping by the PAN layers.

Electrochromic Properties of the LBL Films. The color change of the EC films during the CV measurement originates from the redox process of PANBS (and PAN), which turn dark green and are bleached when oxidized and reduced, respectively. Thus, under the applied potential above 0.5 V, the EC film changed to a dark-green color within 100 ms. The color was intensified as the applied potential was raised to 0.7 V and venerable after the electricity was disconnected. On the other hand, the dark-green color faded when the potential was reversed toward negative. The bleached state was also conserved when the electricity was disconnected. Such an electrical bistability of color change was apparent in the visible spectra resulting in absorbance increase >350 nm when oxidized, as shown in Figure 5a for L1. Absorbance in the visible region was decreased back to baseline when the applied potential was lower than 0 V.

All-solid-state EC devices were assembled using the photopolymerizable electrolyte described in ref 4. When the applied potential was 3.0 V, the all-solid-state EC device was shown to have a dark-green color. On the other hand, the dark-green color faded when the potential was switched to −3 V. The electrical bistability of color change was also observed from the solid-state EC. Figure 5b,c shows UV−visible spectra of the EC devices prepared from L5 and L1 films, respectively. The coloration was more effective with L1 than with L5, possibly due to the color development of the acid-doped PAN in L5 in the oxidized state. The absorbance change of the EC device (ΔOD) between the bleached and colored state to the step potentials of ±3 V, with a switching time of 20 s, for the mixed cationic films (L1−L4) is larger than that of the EC devices prepared with monocationic films (PANBS/PAN and PANBS/VBOD), as compared in Figure 6a. It is important to note that absorbance change (ΔOD) is large in L1 compared to that in other systems in this study. Since ΔOD is directly dependent on the concentration of the electrochemically active species, and the number of PANBS layers is the same for L1−L6, it may be thought that ΔOD relates to the number of PAN layers. The ΔOD of the EC devices, however, was not dependent

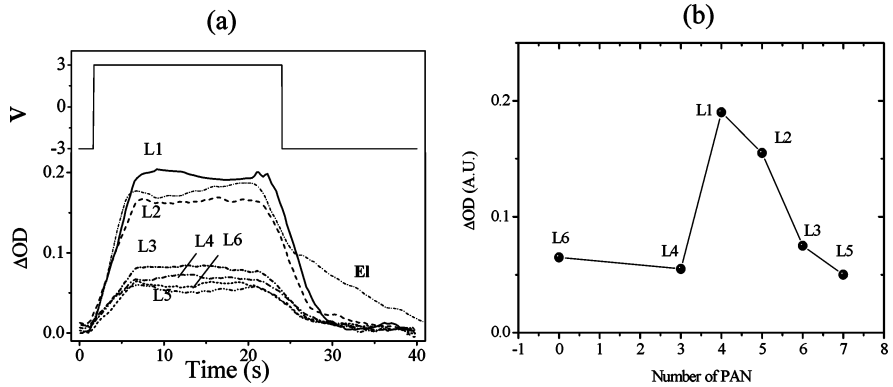

Figure 6. (a) Optical response of EC devices fabricated using the EC films L1−L6 and electrochemically deposited film (El), to step potentials of ±3 V. (b) Plot of the ΔOD of the EC devices to step potentials of ±3 V against the number of PAN layers in each film.

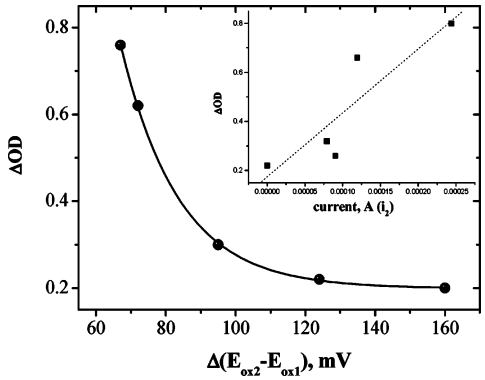

Figure 7. Correlation of potential difference ($E_{ox2} - E_{ox1}$) in Table 1 against ΔOD.

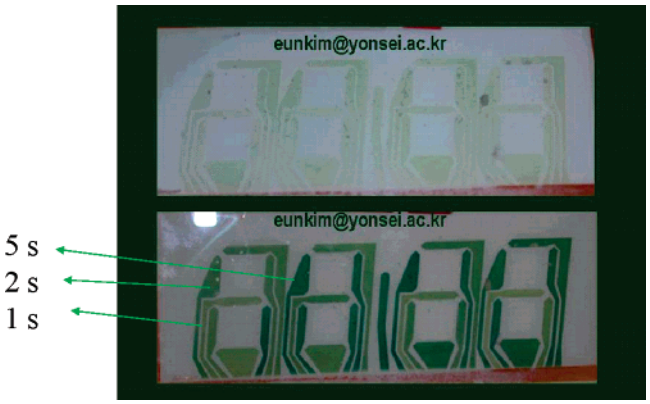

Figure 8. EC response of an all solid-state ECD fabricated using the LBL method, with the layer composition of L1 on a patterned ITO glass.

on the number of PAN layers, as shown in Figure 6b. This result strongly suggests that electrochromic response is highly dependent on the layer composition, which could be related to an interlayer barrier for charge (electron/ion) transport between the conductive layers. The EC responses, particularly in bleaching, of the LBL assembled EC film in the solid state were significantly faster than that of the electrochemically deposited film (El in Figure 6a). This indicates that the LBL method allows fine-tuning of the electroconductive polymer structure when the polymers are assembled, to facilitate electron/ion transport.

Relationship between Electrochromic Response and Interlayer Barrier Potential (E_{ox2}). The facilitated charge transport in the mixed ionic film should be related to the electrochromic response discussed above. The ΔOD was correlated to the current density of the second peak of CV in a linear fashion, as shown in the inset of Figure 7. Most importantly, ΔOD was well correlated with the peak separation (ΔE) between E_{ox1} and E_{ox2}, as shown in Figure 7, with the following relation:

$$\Delta\mathrm{OD} = 1.57 \exp(-\Delta E/16.7) + 0.0099 \qquad (R^2 = 0.9998) \tag{2}$$

This result strongly suggests that the electrochromic response of the LBL assembled EC device is highly dependent on the intermediate energy level generated by the interlayer barrier potential (E_{ox2}) in the mixed cationic layer. It also emphasizes that the EC response of the LBL assembled film could be optimized by the layer composition to reduce ILB.

An all-solid-state EC device was fabricated using a patterned ITO glass, on which PANBS was assembled using the LBL method, as described above. It was then covered with the radiation-curable electrolytes-coated ITO, sealed, and photocured for 30 s under UV light. The EC response of the device is shown in Figure 8. Within 1 s, the color change was detectable, and it became larger within 5 s of voltage application at 3 V. The patterned image was preserved when the electricity was disconnected. The colored pattern was erased as the potential was switched to −2 V, as shown in Figure 8 (top).

In conclusion, the EC films were prepared by the LBL technique, by which the layer sequence could be controlled to optimize electron through the layer. EC films having alternative bilayers of PANBS/PAN and PANBS/VBOD showed high EC response, possibly due to facilitated electron transport by PAN and ion transport by VBOD layer. The electrochemical and EC properties of the films prepared by the LBL technique were characterized. In addition the effect of the bilayer sequence on the EC properties was rationalized by defining interlayer barrier (ILB). Further investigation is in progress to elaborate the redox process, which considers layer-by-layer interface in a mixed ionic LBL assembly. It is hoped that this investigation will shed light on the electronic function in a layered electrochemical structure.

Acknowledgment. We acknowledge the financial support of MOST (the Ministry of Science and Technology), MOCIE (the Ministry of Commerce, Industry, and Energy), and MEHRD (Ministry of Education & Human Resources Development), Korea.

CM051492N